Electrochimica Acta 174 (2015) 456–463

Contents lists available at ScienceDirect

Electrochimica Acta

journal homepage: www.elsevier.com/locate/electacta

Controllable preparation of multi-dimensional hybrid materials of nickel-cobalt layered double hydroxide nanorods/nanosheets on electrospun carbon nanofibers for high-performance supercapacitors

Feili Lai, Yunpeng Huang, Yue-E Miao, Tianxi Liu*

State Key Laboratory of Molecular Engineering of Polymers, Department of Macromolecular Science, Fudan University, Shanghai 200433, PR China

ARTICLE INFO

Article history:
Received 30 March 2015
Received in revised form 7 June 2015
Accepted 7 June 2015
Available online 10 June 2015

Keywords:
nickel-cobalt layered double hydroxides
hierarchical nanostructure
electrospinning
carbon nanofiber membrane
supercapacitors

ABSTRACT

Hybrid nanomaterials with hierarchical structures have been considered as one kind of the most promising electrode materials for high-performance supercapacitors with high capacity and long cycle lifetime. In this work, multi-dimensional hybrid materials of nickel-cobalt layered double hydroxide (Ni-Co LDH) nanorods/nanosheets on carbon nanofibers (CNFs) were prepared by electrospinning technique combined with one-step solution co-deposition method. Carbon nanofiber membranes were obtained by electrospinning of polyacrylonitrile (PAN) followed by pre-oxidation and carbonization. The successful growth of Ni-Co LDH with different morphologies on CNF membrane by using two kinds of auxiliary agents reveals the simplicity and universality of this method. The uniform and immense growth of Ni-Co LDH on CNFs significantly improves its dispersion and distribution. Meanwhile the hierarchical structure of carbon nanofiber@nickel-cobalt layered double hydroxide nanorods/nanosheets (CNF@Ni-Co LDH NR/NS) hybrid membranes provide not only more active sites for electrochemical reaction but also more efficient pathways for electron transport. Galvanostatic charge-discharge measurements reveal high specific capacitances of 1378.2 F g^{-1} and 1195.4 F g^{-1} (based on Ni-Co LDH mass) at 1 A g^{-1} for CNF@Ni-Co LDH NR and CNF@Ni-Co LDH NS hybrid membranes, respectively. Moreover, cycling stabilities for both hybrid membranes are significantly enhanced compared with those of Ni-Co LDH NR and NS powders. This facile method provides a new strategy for designs and applications of binary transition metal oxides/hydroxides deposited on various substrates for next-generation energy storage devices.

1. Introduction

Nowadays, high-performance energy storage technologies are widely explored in order to remit the increasingly tensive energy situation [1,2]. Supercapacitors, also called as electrochemical capacitors, have attracted extensive attention because of their fast charge-discharge process, long lifespan and high power density [3–7]. In general, supercapacitors can be divided into two categories of electrical double-layer capacitors (EDLCs) and pseudocapacitor based on their charge-discharge mechanism [6,8]. Electrode materials for EDLCs, such as reduced graphene oxide, carbon nanotubes and graphitized carbon, usually own good cycle lifetime but low specific capacity to meet the ever-growing needs for high-performance energy devices [9–11]. Transition-metal oxides/hydroxides, such as RuO_2, MnO_2, NiO, $Ni(OH)_2$, Co_3O_4, Fe_3O_4 and their binary systems are typical electrode materials for pseudocapacitors with a relatively high specific capacity [12–18]. Nickel-cobalt layered double hydroxides (Ni-Co LDHs) are one kind of the most promising candidates among binary metal hydroxides due to their low cost, high redox activity and electrical conductivity [19–22]. Moreover, abundant OH^- ions in hydrotalcite-like structure of Ni-Co LDHs can drastically increase the ion exchange rate during the electrochemical charge-discharge processes. Xie et al. synthesized Co-Ni layered double hydroxide (Co_xNi_{1-x} LDH) nanoparticles by a poly (vinyl pyrrolidone)-assisted chemical co-precipitation method, which exhibited the highest specific capacitance of 2614 F g^{-1} when the atomic ratio of Co to Ni was equal to 0.57:0.43 [23]. Hsu et al. obtained mesoporous Ni-Co oxy-hydroxides through the microwave assisted hydrothermal annealing method, showing a specific capacitance of 636 F g^{-1} under the calcination temperature of 200 °C [24]. Though high specific capacitance was achieved, the low electrochemical stability can hardly be avoided for bulk Ni-Co LDH due to the conglomeration of nanoparticles, which severely limits their wider applications.

It has been proven that hybrid structures of Ni-Co LDHs and carbonaceous materials, such as CNT/Ni-Co oxides composites

* Corresponding author. Tel.: +86 21 55664197; fax: +86 21 65640293.
E-mail address: txliu@fudan.edu.cn (T. Liu).

http://dx.doi.org/10.1016/j.electacta.2015.06.031
0013-4686/

[25], reduced graphene oxides/Ni-Co nanostructures [26,27], glassy carbon/Co-Ni films [28], can greatly contribute to the optimization of electrode properties with better rate/cycling stability and higher specific capacitance. Salunkhe et al. developed nickel-cobalt binary metal hydroxide nanorods coated multi-walled carbon nanotube hybrid material through a chemical synthesis method [29]. The as-obtained hybrid showed enhanced supercapacitive performance and cycling ability. Huang et al. synthesized a series of three-dimensional nanocomposite electrodes by facile electro-deposition of cobalt and nickel double hydroxide nanosheets on porous $NiCo_2O_4$ nanowires which were grown on carbon fiber paper for high-performance supercapacitors, showing high rate capability and excellent cycling stability [30]. Chen et al. also fabricated Ni-Co LDHs on macroporous nickel foam by one-step hydrothermal co-deposition method [31]. The as-obtained Ni-Co LDH hybrid films exhibit ultra-high specific capacitance of 2682 F g^{-1} at 3 A g^{-1} (based on active materials) and energy density of 77.3 Wh kg^{-1} at 623 W kg^{-1}, making the Ni-Co LDH hybrid films promising electrode materials for high-performance supercapacitors. Despite the excellent electrochemical performance, most of the above hybrid materials need to be blended with conductive and binding agents as electrodes. The electrode materials thus obtained can hardly be flexible enough to meet tough environmental situations. In addition, the cumbersome process with introduction of excess binding agents may severely affect the electrochemical performance. Therefore, it is necessary to develop flexible electrode materials for high-performance supercapacitor applications.

As an effective method to build one-dimensional nanostructures, electrospinning technique attracts lots of attention, through which micron-sized or even nano-sized fibers can be easily generated [32–39]. Free-standing electrospun nanofiber membranes have many outstanding characteristics such as large specific surface area, controllable diameter and excellent flexibility, making them ideal candidates for tissue engineering, drug carrier, heavy metal removal, as well as electrode materials for Li-ion batteries and supercapacitors [40–43]. Kim et al. synthesized the carbon nanofiber webs from polyacrylonitrile solutions, which possess high specific surface area and huge conductive network of nano-sized fibers as a new type supercapacitor electrode [44]. Therefore, electrospun carbon nanofiber (CNF) membrane will be a promising template for the next-generation energy storage materials.

In this study, PAN nanofiber membranes were firstly fabricated by electrospinning with an average diameter of 300-450 nm, followed by a two-stage heat treatment of pre-oxidation and high temperature carbonization to obtain CNF membranes. With virtue of two different auxiliary agents (urea and hexamethylenetetramine), Ni-Co LDH nanorods (Ni-Co LDH NR) and ultrathin Ni-Co LDH nanosheets (Ni-Co LDH NS) were successfully grown on the surface of CNFs to form multi-dimensional structure of CNF@Ni-Co LDH hybrids by a one-step solution co-deposition method. The hierarchical nanostructures of CNF@Ni-Co LDH hybrid membranes can effectively improve the dispersion of Ni-Co LDH nanoparticles, increase the specific surface area and provide more active sites for electrolyte ion adsorption and transport. Electrochemical results show remarkably enhanced capacitive performance with the specific capacitance of 1378.2 F g^{-1} and 1195.4 F g^{-1} (based on the mass of Ni-Co LDHs) at 1 A g^{-1} for CNF@Ni-Co LDH NR and CNF@Ni-Co LDH NS membranes, respectively. Therefore, this method suggests a facile and universal approach to construct binary transition metal oxides/hydroxides and carbonaceous hybrid materials with hierarchical nanostructures for high-performance supercapacitor electrodes.

2. Experimental

2.1. Materials

Polyacrylonitrile (PAN, Mw = 150,000 g mol^{-1}) was purchased from Sigma-Aldrich. Nickel nitrate hexahydrate ($Ni(NO_3)_2 \cdot 6H_2O$) was purchased from Aladdin Chemical Reagent Co. Cobalt nitrate hexahydrate ($Co(NO_3)_2 \cdot 6H_2O$), urea, hexamethylenetetramine (HMT), *N,N*-dimethylformamide (DMF), sodium hydroxide (NaOH) and sulfuric acid (H_2SO_4) were all purchased from Sinopharm Chemical Reagent Co. All of the chemicals were of analytic grade and used without further purification.

2.2. Preparation of electrospun CNF membranes

PAN was dissolved in DMF under magnetic stirring at room temperature for 12 h to prepare a 10 wt % spinning solution, which was loaded into a 5 mL syringe with a stainless steel needle having an inner diameter of 0.5 mm. A high voltage of 15 kV and a feeding rate of 1 mL h^{-1} were applied to the spinneret. The electrospun PAN nanofibers were collected onto the rotating aluminum collector, which was placed 15 cm away from the spinneret. The collected PAN nanofiber membranes underwent pre-oxidation by the following program: heating up to 250 °C at a ramp rate of 2 °C min^{-1}, followed by holding at 250 °C for 2 h. Afterwards, PAN

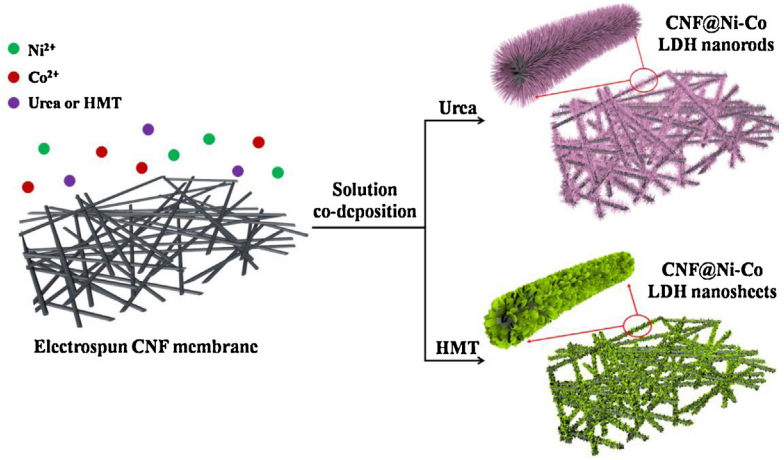

Fig. 1. Schematic illustration of the preparation of CNF@Ni-Co LDH NR and CNF@Ni-Co LDH NS hybrid membranes.

nanofiber membranes were carbonized in a nitrogen flow (to obtain carbon nanofiber membranes): heating up to 950 °C at a ramp rate of 3 °C min^{-1}, then holding for 0.5 h.

2.3. Preparation of CNF@Ni-Co LDH hybrid membranes

The typical procedure for preparing CNF@Ni-Co LDH hybrid membranes is shown in Fig. 1. Briefly, the electrospun CNF membrane ($2 \times 5\ cm^2$) was firstly immersed into concentrated sulfuric acid for 0.5 h to increase its hydrophilicity, then washed with deionized water for several times. For the preparation of CNF@Ni-Co LDH NR membrane, the electrospun CNF membrane was firstly immersed into a transparent pink solution of 0.7 mmol $Ni(NO_3)_2{\cdot}6H_2O$, 1.4 mmol $Co(NO_3)_2{\cdot}6H_2O$ and 12 mmol urea in the mixed solvent of 20 mL ethanol and 20 mL deionized water at room temperature, followed by heating to 80 °C in an oil bath for 6 h. Then, the obtained CNF@Ni-Co LDH NR membrane was cleaned by deionized water and ethanol for several times to remove the by-products on the surface, and dried at 70 °C for 24 h.

Similarly, the acidized CNF membrane ($2 \times 5\ cm^2$) was immersed into the mixed solution of 0.5 mmol $Ni(NO_3)_2{\cdot}6H_2O$, 1.0 mmol $Co(NO_3)_2{\cdot}6H_2O$ and 5 mmol HMT in 20 mL ethanol and 20 mL deionized water at room temperature, followed by heating to 80 °C in an oil bath for 8 h to obtain CNF@Ni-Co LDH NS membrane. It should be noted that both urea and HMT were used here as the auxiliary growth agents to regulate the morphology of Ni-Co LDH.

For comparison, Ni-Co LDH nanorod and nanosheet powdery samples were respectively synthesized by the same approach, where pink and light green precipitates were successfully obtained after the reactions at 80 °C in oil bath. Finally, the products were cleaned in water and isolated by centrifugation, and dried at 70 °C for 24 h.

2.4. Characterization

Morphologies of CNF@Ni-Co LDH NR and NS membranes were observed by field-emission scanning electron microscope (FESEM, Ultra 55, Zeiss) at a high tension of 5 kV. Phase structures of the samples were measured by X-ray diffraction (XRD, X'pert PRO, PANalytical) with Cu Kα radiation (λ = 0.1542 nm) at an angular speed of (2θ) 5° min^{-1}. The chemical compositions of the samples were examined by X-ray photoelectron spectroscopy (XPS) on a RBD upgraded PHI-5000C ESCA system (Perkin Elmer) with K (1486.6 eV) as X-ray source. All XPS spectra were corrected according to the C1s line at 285.0 eV. Curve fitting and background subtraction were accomplished using the RBD AugerScan 3.21 software provided by RBD Enterprises. Thermogravimetric analysis (TGA, Pyris 1 TGA, PerkinElmer) was performed in air from 100 to 700 °C at a heating rate of 10 °C min^{-1} in order to measure the mass content of Ni-Co LDH in the hybrid membranes.

2.5. Electrochemical measurements

All the electrochemical measurements were performed in 1 M NaOH solution on an electrochemical working station (CHI660D, Chenhua Instruments Co. Ltd., Shanghai), where the as-prepared

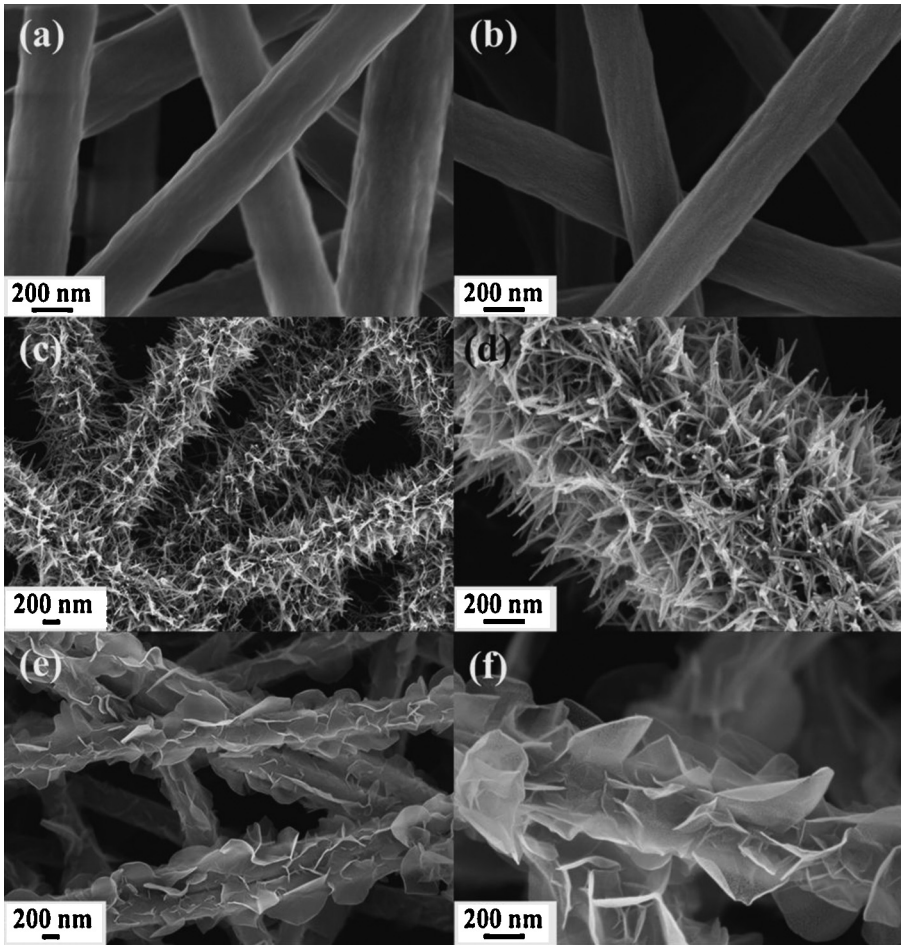

Fig. 2. Typical FESEM images of (a) electrospun PAN non-woven membrane; (b) bare carbon nanofibers; (c, d) CNF@Ni-Co LDH NR hybrid nanostructure at different magnifications; (e,f) CNF@Ni-Co LDH NS hybrid nanostructure at different magnifications.

CNF@Ni-Co LDH hybrid membrane (~0.20 mg) was directly used as the working electrode, Pt wire and Ag/AgCl as the counter and reference electrode, respectively. Cyclic voltammograms (CV) were recorded between 0 and 0.5 V at different scan rates ranging from 5 to 100 mV s^{-1}. Galvanostatic charge-discharge testing was measured between 0 and 0.4 V under different current densities from 1 to 10 A g^{-1}. Electrochemical impedance spectroscopy (EIS) measurement was conducted by applying an AC voltage in the frequency range between 100 kHz and 10 mHz with 5 mV amplitude.

The specific capacitance (C) of the electrode can be calculated from galvanostatic charge-discharge tests using the following equation:

$$C = \frac{I \times \Delta t}{m \times \Delta v} \quad (1)$$

Where C (F g^{-1}) is the specific capacitance of the electrode based on active materials, I (A) is the discharge current, Δt (s) is the discharge time, Δv (V) is the discharge potential window, and m (g) is the mass of active materials, respectively.

3. Results and discussions

3.1. Morphological and structural characterization

Fig. 2a shows the FESEM image of electrospun PAN nanofiber membrane, which exhibits uniform fiber diameter of about 300-450 nm and smooth surface with no beads and breakages. After pre-oxidation and carbonization treatments, CNF membrane with decreased fiber diameter of 250-350 nm is obtained (Fig. 2b), which is caused by the pyrogenic decomposition and cyclization reaction of PAN molecular chains. Furthermore, the thickness of thus obtained membranes is about 17.16 ± 0.13 μm as shown in Fig. S1. The randomly oriented CNFs result in micron-porous meshes, which are beneficial for the penetration of reaction solutions, thus realize the uniform and immense growth of different nanostructures of Ni-Co LDH. Fig. 2c and 2d show FESEM images of CNF@Ni-Co LDH NR hybrid membrane at low and high magnifications, respectively. As can be observed, the surface of CNFs is covered by uniformly and immensely distributed Ni-Co LDH nanorods with length of about 600 nm after the solution co-deposition treatment. Hierarchical architecture of CNF@Ni-Co LDH NS hybrid membrane is also easily obtained by replacing urea with HMT during the synthesis process, revealing the universality of this method. It can be seen that ultrathin LDH nanosheets are uniformly anchored on the surface of CNFs, as shown in Fig. 2e and f. These hierarchically organized hybrid nanostructures could undoubtedly reduce the aggregation of pure Ni-Co LDH (Fig. S2), provide high specific surface area and numerous active sites, which can help gather ions from electrolyte and thus improve the electrochemical performance of CNF@Ni-Co LDH hybrid membrane electrodes.

XRD patterns are collected to characterize the crystalline structures of all the samples, as shown in Fig. 3. Almost no peak can be observed for the bare CNFs, indicating an amorphous structure. Four distinct diffraction peaks located at 2θ = 12.2°, 24.4°, 33.4°, 37.8° for CNF@Ni-Co LDH NR hybrid membrane can be indexed to (0 0 3), (0 0 6), (0 0 9) and (0 1 5) planes of hydrotalcite-like LDHs, implying successful immobilized growth of Ni-Co LDH nanorods on the surface of CNFs [45]. On the other hand, a slight shift of the diffraction peaks can be observed for both Ni-Co LDH NS powdery sample and CNF@Ni-Co LDH NS hybrid membrane, probably due to different uploading mole ratios of Ni:Co resulting from the effects of different auxiliary agents during the reactions. According to the previous study, a gradual transformation of crystal structure can be observed with different Ni:Co mole ratios [31].

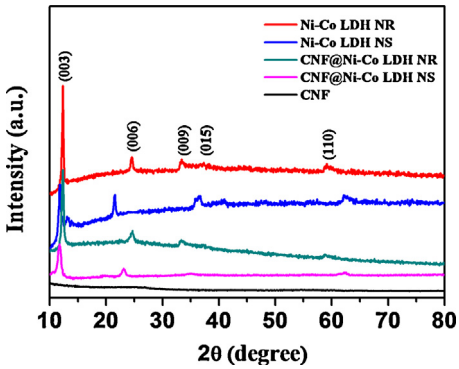

Fig. 3. XRD patterns of CNF membrane, Ni-Co LDH NR and Ni-Co LDH NS powders, CNF@Ni-Co LDH NR and CNF@Ni-Co LDH NS hybrid membranes.

Further insights into the surface information of the hybrid membranes are obtained from XPS spectra, as shown in Fig. 4. The survey spectrum (0-1000 eV) mainly shows carbon (C 1s) and oxygen (O 1s) species. In Ni 2p spectrum of CNF@Ni-Co LDH NS hybrid membrane (Fig. 4b), two obvious shakeup satellites at 874.8 eV and 856.7 eV can be respectively identified as Ni $2p_{1/2}$ and Ni $2p_{3/2}$ signals of Ni^{2+} [46]. As shown in Fig. 4c, the Co 2p lines are split into two peaks: Co $2p_{1/2}$ (797.7 eV) and Co $2p_{3/2}$ (782.4 eV) [47]. These XPS results further confirm the successful synthesis of CNF@Ni-Co LDHs.

TGA tests are conducted to further analyze the content of Ni-Co LDH on the CNF membrane, as shown in Fig. 5. The average mass loading of Ni-Co LDH NR and NS on CNF membrane are respectively calculated to be 63.34% and 50.65% as listed in Table 1, revealing a high mass loading of Ni-Co LDH on the CNF membranes, which is beneficial to a better capacitive performance.

3.2. Electrochemical properties

Electrochemical measurements were performed with a standard three-electrode system in 1 M NaOH solution to evaluate the electrochemical performance of thus obtained hybrid electrode materials. Fig. 6 shows the typical CV curves of CNF membrane, Ni-Co LDH NR and Ni-Co LDH NS powders, CNF@Ni-Co LDH NR and CNF@Ni-Co LDH NS hybrid membranes. The comparisons in Fig. 6a and b clearly reveal much higher capacitances of CNF@Ni-Co LDH NR/NS hybrid membranes than those of Ni-Co LDH NR/NS powders and CNF membrane, indicating excellent pseudocapacitive performance and fine dispersion of Ni-Co LDH on the surface of CNFs.

In addition, the mechanism of the improved capacitive behavior is probably due to the effective electron transfer paths during the charge-discharge process, as proposed in Fig. 7. The conductive network formed by non-woven electrospun CNF membranes can undoubtedly provide an enormous and efficient pathway for the electron transportation [48]. Besides, the uniform and immense growth of Ni-Co LDH nanorods and nanosheets on the surface of CNFs (as shown in Fig. 2) can significantly increase the specific surface area of the hybrid membrane electrode materials, which can benefit the following Faradaic reactions of $Ni_xCo_y(OH)_z$ [49]:

$$(2)Ni_xCo_y(OH)_z + OH^- \leftrightarrow NiOOH + CoOOH + H_2O + e^-$$

$$(3)CoOOH + OH^- \leftrightarrow CoO_2 + H_2O + e^-$$

Furthermore, an intimate electronic transmission channel can be effectively constructed between the interface of CNFs and Ni-Co LDHs through the physical interaction force. Therefore, these hierarchical nanostructures can not only provide deep electrolyte penetration for OH^- but also construct a multilevel conductive

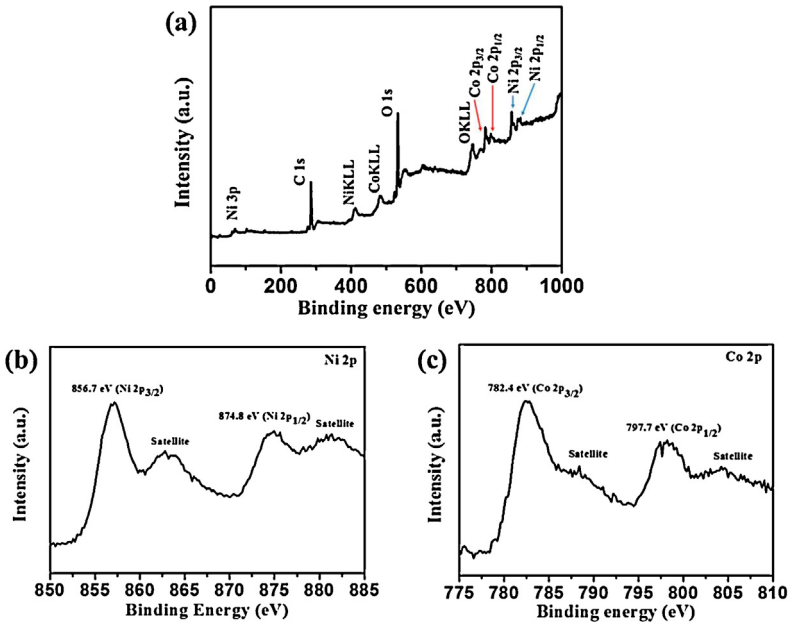

Fig. 4. XPS spectra of CNF@Ni-Co LDH NS hybrid membrane: (a) the full survey scan, (b) Ni 2p region, and (c) Co 2p region.

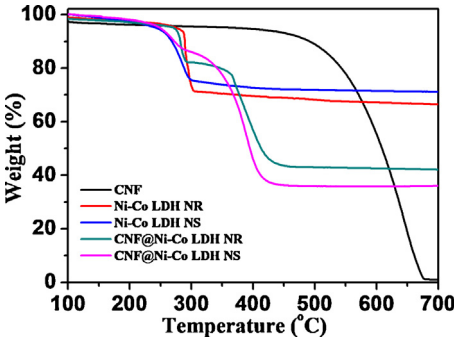

Fig. 5. TGA profiles of CNF membrane, Ni-Co LDH NR and Ni-Co LDH NS powders, CNF@Ni-Co LDH NR and CNF@Ni-Co LDH NS hybrid membranes under air flow at a temperature ramp of 10 °C min^{-1}.

network for electron transportation, which will efficiently and drastically improve the electrochemical performance.

Fig. 8a and b show the typical CV curves of CNF@Ni-Co LDH NR and NS hybrid membranes under various sweep rates ranging from 5 to 100 mV s^{-1}, respectively. A pair of redox peaks can be observed within the potential range from 0 to 0.5 V, revealing the pseudocapacitive characteristics mainly from the Faradaic redox reactions of M-O/M-O-OH (where M refers to Ni or Co) [50]. An obviously increasing shift of the peaks to higher potentials and a rising of the current density are resulted from the inefficient transportation of OH^- with the increase of scan rate, which will limit the above Faradaic reactions of $Ni_xCo_y(OH)_z$. Fig. 8c and d show the galvanostatic charge-discharge curves of CNF@Ni-Co LDH NR and NS hybrid membranes between 0 and 0.4 V under different current densities. A voltage plateaus around 0.15-0.2 V and an almost symmetric shape are observed for both hybrid

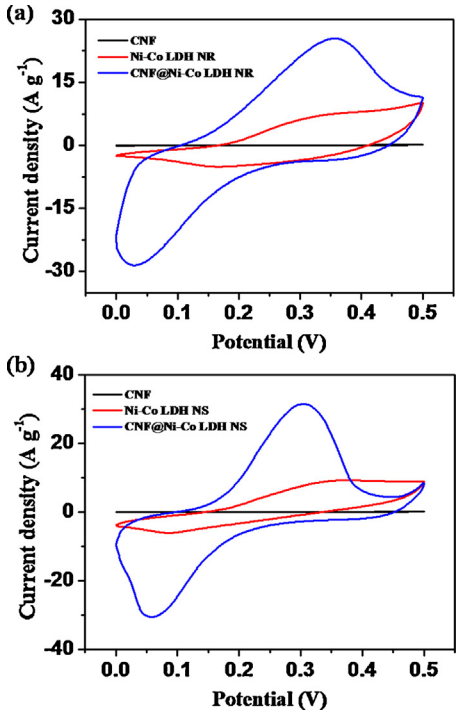

Fig. 6. CV curves of (a) CNF membrane, Ni-Co LDH NR powder and CNF@Ni-Co LDH NR hybrid membrane; (b) CNF membrane, Ni-Co LDH NS powder and CNF@Ni-Co LDH NS membrane at a scan rate of 20 mV s^{-1}.

membrane electrode materials during the charge-discharge processes, which is consistent with the previous reports [51]. The specific capacitances calculated by Eq. (1) (based on active

Table 1
TGA results of the samples.

Sample	CNF	Ni-Co LDH NR	Ni-Co LDH NS	CNF@Ni-Co LDH NR	CNF@Ni-Co LDH NS
Residue mass (%)	1.0%	66.4%	71.2%	42.1%	36.1%
LDH content (%)	–	100%	100%	63.3%	50.6%

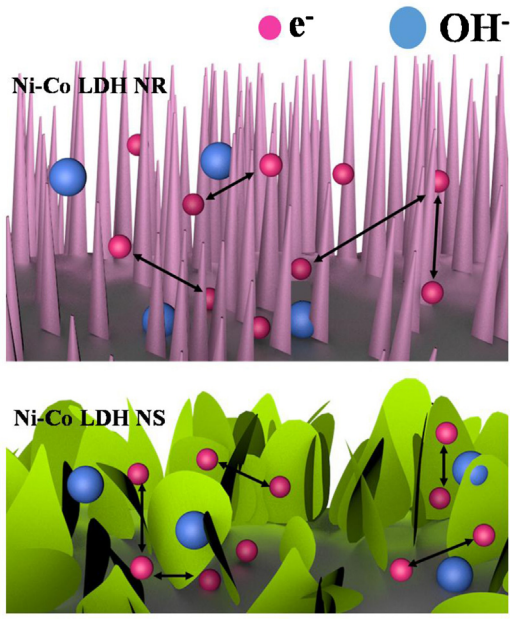

Fig. 7. The illustration of electron transfer processes in CNF@Ni-Co LDH NR and CNF@Ni-Co LDH NS hybrid membranes during the electrochemical reactions.

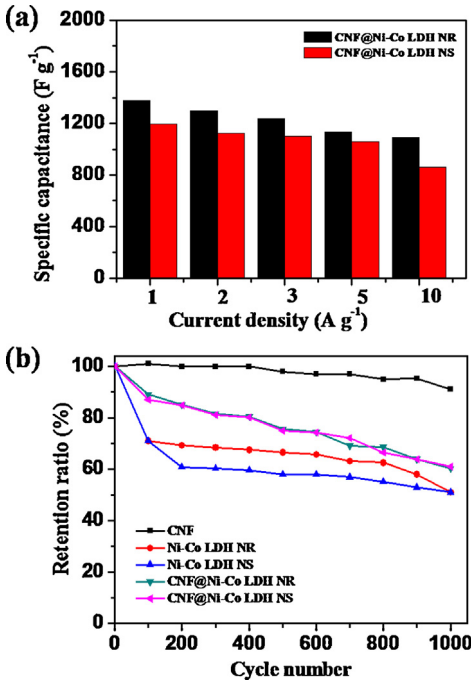

Fig. 9. (a) Specific capacitance of CNF@Ni-Co LDH NR and CNF@Ni-Co LDH NS hybrid membranes at different discharge current densities. (b) Cycling performance of CNF membrane, Ni-Co LDH NR and Ni-Co LDH NS powders, CNF@Ni-Co LDH NR and CNF@Ni-Co LDH NS hybrid membranes at constant current density of 5 A g^{-1}.

material) are 1378.2, 1297.5, 1238.0, 1131.9and 1089.5 F g^{-1} for CNF@Ni-Co LDH NR hybrid membrane at the discharge current densities of 1, 2, 3, 5 and 10 A g^{-1}, respectively. In the same way, the specific capacitances of CNF@Ni-Co LDH NS hybrid membrane are calculated to be 1195.4, 1125.9, 1102.0, 1056.3, 858.8 F g^{-1} (based on active material) at the discharge current densities of 1, 2, 3, 5 and 10 A g^{-1}, respectively. These values of thus obtained hybrid membranes are higher than those (about 902 F g^{-1} at a current density of 2 A g^{-1}) reported by Lou et al. for powdery materials of hierarchical hybrids nanostructures composed of $NiCo_2O_4$ on carbon nanofibers [21], which is mainly attributed to continuous and three-dimensional template of electrospun carbon nanofibers instead of synthetic carbon nanofibers through hydrothermal method. Moreover, the layered laminated nanostructure of Ni-Co LDH can much efficiently contribute to the ion transport than $NiCo_2O_4$ during electrochemical processes. Fig. 9a presents the relationship between specific capacitance and current density, showing 79.1% and 71.8% capacitance retention at 10 A g^{-1} for CNF@Ni-Co LDH NR and CNF@Ni-Co LDH NS hybrid membranes respectively, which reveals a high rate stability of the hybrid electrodes. The cycling stability within 1000 cycles was evaluated by the charge-discharge measurements at a constant current density of 5 A g^{-1}, as shown in Fig. 9b. The CNF membrane presents a low capacitance loss of about 8.9% after 1000 cycles, showing a good cycling stability. A slight increase of the

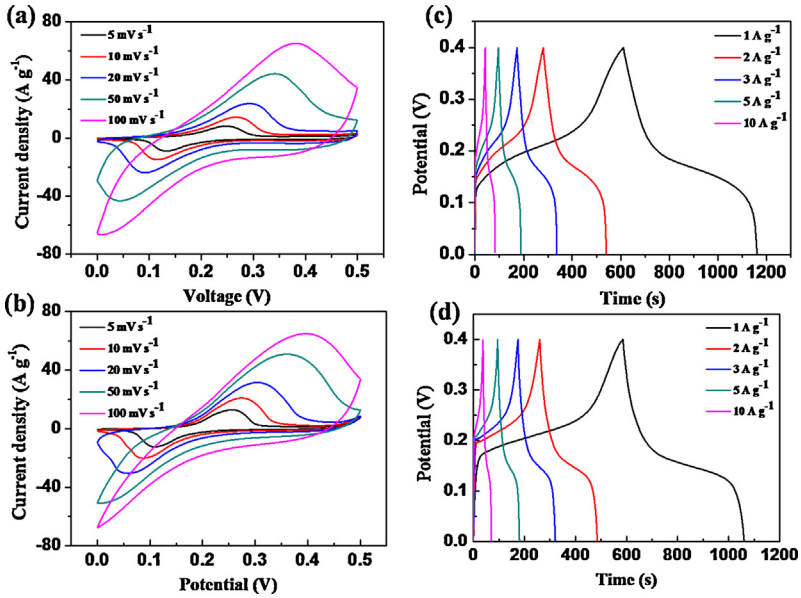

Fig. 8. CV curves of (a) CNF@Ni-Co LDH NR and (b) CNF@Ni-Co LDH NS hybrid membranes at different scan rates from 5 to 100 mV s^{-1}; Galvanostatic charge-discharge curves of (c) CNF@Ni-Co LDH NR and (d) CNF@Ni-Co LDH NS hybrid membranes at different current densities.

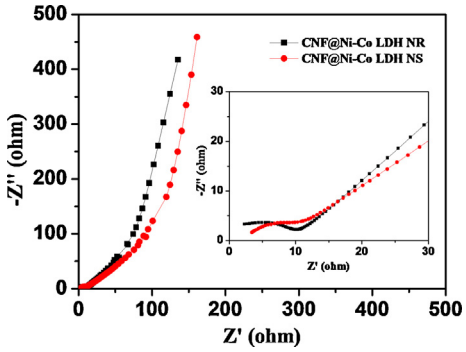

Fig. 10. Nyquist plots of CNF@Ni-Co LDH NR and NS hybrid membranes obtained at open circuit potentials.

capacitance retention (about 60.3% and 61.0%, respectively) can be observed for CNF@Ni-Co LDH NR and CNF@Ni-Co LDH NS hybrid membranes, compared with those (about 51.1% and 52.1%, respectively) for Ni-Co LDH NR and NS powders. Since the intrinsic electrical double-layer capacitor characteristics of CNFs result in a better cycling stability while Ni-Co LDH holds a high pseudocapacitance, the nanostructured hybrid electrodes integrate respective advantages of electrical double-layer capacitor and pseudocapacitor, thus giving birth to an outstanding electrochemical performance for CNF@Ni-Co LDH hybrid electrode materials.

As shown in Fig. 10, Nyquist plots of CNF@Ni-Co LDH NR and NS hybrid membranes are obtained in the frequency range of 100 kHz to 10 mHz at the open circuit potentials. The vertical slope of the linear part in the low frequency region indicates low diffusion resistance of ion and electron transfer in both CNF@Ni-Co LDH NR and NS hybrid membranes, meanwhile the small semicircle diameters imply low interfacial resistance in the electrochemical system.

4. Conclusions

In summary, Ni-Co LDH nanorods and nanosheets have been grown on electrospun carbon nanofiber by a one-step solution co-deposition method with aid of two different auxiliary agents to form multi-dimensional hybrid materials of CNF@Ni-Co LDH NR and NS. These two hybrid membrane electrodes respectively exhibit high specific capacitance of 1378.2 F g^{-1} and 1195.4 F g^{-1} at a current density of 1 A g^{-1} and a higher cycling stability than Ni-Co LDH NR and NS powders. The integration of conductive CNF membranes with electrochemical active Ni-Co LDH NR and NS provides significantly improved specific surface area and fully exposed active sites for the high capacitive performance. Moreover, this method can be extended to the synthesis of other carbon nanofiber@bimetallic nanostructure hybrid membranes for high-performance supercapacitors.

Acknowledgement

The authors are grateful for the financial support from the <GS1>National Natural Science Foundation of China (51125011, 51373037, 51433001).

Appendix A. Supplementary data

Supplementary data associated with this article can be found, in the online version, at http://dx.doi.org/10.1016/j.electacta.2015.06.031.

References

[1] X.Y. Dong, L. Wang, D. Wang, C. Li, J. Jin, Layer-by-layer engineered Co-Al hydroxide nanosheets/graphene multilayer films as flexible electrode for supercapacitor, Langmuir 28 (2012) 293–298.
[2] J.M. Tarascon, M. Armand, Issues and challenges facing rechargeable lithium batteries, Nature 414 (2001) 359–367.
[3] M.M. Shaijumon, F.S. Ou, L.J. Ci, P.M. Ajayan, Synthesis of hybrid nanowire arrays and their application as high power supercapacitor electrodes, Chem. Commun. (2008) 2373–2375.
[4] A. Burke, Ultracapacitors: why, how, and where is the technology, J. Power Sources 91 (2000) 37–50.
[5] A.S. Arico, P. Bruce, B. Scrosati, J.M. Tarascon, W. Van Schalkwijk, Nanostructured materials for advanced energy conversion and storage devices, Nat. Mater 4 (2005) 366–377.
[6] P. Simon, Y. Gogotsi, Materials for electrochemical capacitors, Nat. Mater 7 (2008) 845–854.
[7] J.R. Miller, P. Simon, Materials science—electrochemical capacitors for energy management, Science 321 (2008) 651–652.
[8] J.C. Huang, T. Lei, X.P. Wei, X.W. Liu, T. Liu, D.X. Cao, J.L. Yin, G.L. Wang, Effect of Al-doped beta-$Ni(OH)_2$ nanosheets on electrochemical behaviors for high performance supercapacitor application, J. Power Sources 232 (2013) 370–375.
[9] K.H. An, W.S. Kim, Y.S. Park, Y.C. Choi, S.M. Lee, D.C. Chung, D.J. Bae, S.C. Lim, Y. H. Lee, Supercapacitors using single-walled carbon nanotube electrodes, Adv. Mater. 13 (2001) 497 499.
[10] Y. Chen, X. Zhang, D.C. Zhang, P. Yu, Y.W. Ma, High performance supercapacitors based on reduced graphene oxide in aqueous and ionic liquid electrolytes, Carbon 49 (2011) 573–580.
[11] S.J. He, X.W. Hu, S.L. Chen, H. Hu, M. Hanif, H.Q. Hou, Needle-like polyaniline nanowires on graphite nanofibers: hierarchical micro/nano-architecture for high performance supercapacitors, J. Mater. Chem. 22 (2012) 5114–5120.
[12] H.L. Wang, H.S. Casalongue, Y.Y. Liang, H.J. Dai, $Ni(OH)_2$ nanoplates grown on graphene as advanced electrochemical pseudocapacitor materials, J. Am. Chem. Soc. 132 (2010) 7472–7477.
[13] B.J. Li, H.Q. Cao, J. Shao, M.Z. Qu, J.H. Warner, Superparamagnetic Fe_3O_4 nanocrystals@graphene composites for energy storage devices, J. Mater. Chem. 21 (2011) 5069–5075.
[14] R.N. Reddy, R.G. Reddy, Synthesis and electrochemical characterization of amorphous MnO_2 electrochemical capacitor electrode material, J. Power Sources 132 (2004) 315–320.
[15] F. Cao, G.X. Pan, X.H. Xia, P.S. Tang, H.F. Chen, Synthesis of hierarchical porous NiO nanotube arrays for supercapacitor application, J. Power Sources 264 (2014) 161–167.
[16] J. Gomez, E.E. Kalu, High-performance binder-Free Co-Mn composite oxide supercapacitor electrode, J. Power Sources 230 (2013) 218–224.
[17] C.C. Hu, K.H. Chang, M.C. Lin, Y.T. Wu, Design and tailoring of the nanotubular arrayed architecture of hydrous RuO_2 for next generation supercapacitors, Nano Lett. 6 (2006) 2690–2695.
[18] J.L. Zhang, J.C. Fu, J.W. Zhang, H.B. Ma, Y.M. He, F.S. Li, E.Q. Xie, D.S. Xue, H.L. Zhang, Y. Peng, Co@Co_3O_4 core-shell three-dimensional nano-network for high-performance electrochemical energy storage, Small 10 (2014) 2618–2624.
[19] G.Q. Zhang, H.B. Wu, H.E. Hoster, M.B. Chan-Park, X.W. Lou, Single-crystalline $NiCo_2O_4$ nanoneedle arrays grown on conductive substrates as binder-free electrodes for high-performance supercapacitors, Energy Environ. Sci. 5 (2012) 9453–9456.
[20] J.H. Deng, J.C. Deng, Z.L. Liu, H.R. Deng, B. Liu, Capacitive characteristics of Ni-Co oxide nano-composite via coordination homogeneous co-precipitation method, J. Mater. Sci. 44 (2009) 2828–2835.
[21] G.Q. Zhang, X.W. Lou, Controlled growth of $NiCo_2O_4$ nanorods and ultrathin nanosheets on carbon nanofibers for high-performance supercapacitors, Sci. Rep. 3 (2013) 1470.
[22] D.D. Xia, H.C. Chen, J.J. Jiang, L. Zhang, Y.D. Zhao, D.Q. Guo, J.W. Yu, Facilely synthesized α phase nickel–cobalt bimetallic hydroxides: Tuning the composition for high pseudocapacitance, Electrochim. Acta 156 (2015) 108–114.
[23] L.J. Xie, Z.A. Hu, C.X. Lv, G.H. Sun, J.L. Wang, Y.Q. Li, H.W. He, J. Wang, K.X. Li, Co_xNi_{1-x} double hydroxide nanoparticles with ultrahigh specific capacitances as supercapacitor electrode materials, Electrochim. Acta 78 (2012) 205–211.
[24] H. Hsu, K. Chang, R.R. Salunkhe, C. Hsu, C. Hu, Synthesis and characterization of mesoporous Ni-Co oxy-hydroxides for pseudocapacitor application, Electrochim. Acta 94 (2013) 104–112.
[25] A. Arvintea, A.M. Sesayb, V. Virtanenb, Carbohydrates electrocatalytic oxidation using CNT–NiCo-oxide modified electrodes, Talanta 84 (2011) 180–186.
[26] L. Wang, X.P. Lu, Y.J. Ye, L.L. Sun, Y.H. Song, Nickel-cobalt nanostructures coated reduced graphene oxide nanocomposite electrode for nonenzymatic glucose biosensing, Electrochim. Acta 114 (2013) 484–493.
[27] X.Q. Cai, X.P. Shen, L.B. Ma, Z.Y. Jia, C. Xu, A.H. Yuan, Solvothermal synthesis of NiCo-layered double hydroxide nanosheets decorated on RGO sheets for high performance supercapacitor, Chem. Eng. J. 268 (2015) 251–259.
[28] Q.S. Chen, Z.Y. Zhou, G.C. Guo, S.G. Sun, Electrodeposition of nanostructured CoNi thin films and their anomalous infrared properties, Electrochim. Acta 113 (2013) 694–705.

[29] R.R. Salunkhe, K. Jang, S. Lee, S. Yu, H. Ahn, Binary metal hydroxide nanorods and multi-walled carbon nanotube composites for electrochemical energy storage applications, J. Mater. Chem. 22 (2012) 21630–21635.
[30] L. Huang, D.C. Chen, Y. Ding, S. Feng, Z.L. Wang, M.L. Liu, Nickel-cobalt hydroxide nanosheets coated on $NiCo_2O_4$ nanowires grown on carbon fiber paper for high-performance pseudocapacitors, Nano Lett. 13 (2013) 3135–3139.
[31] H. Chen, L.F. Hu, M. Chen, Y. Yan, L.M. Wu, Nickel-cobalt layered double hydroxide nanosheets for high- performance supercapacitor electrode materials, Adv. Funct. Mater. 21 (2014) 934–942.
[32] S. Cavaliere, S. Subianto, I. Savych, D.J. Jones, J. Roziere, Electrospinning: designed architectures for energy conversion and storage devices, Energy Environ. Sci. 4 (2011) 4761–4785.
[33] Z.X. Dong, S.J. Kennedy, Y.Q. Wu, Electrospinning materials for energy-related applications and devices, J. Power Sources 196 (2011) 4886–4904.
[34] C. Kim, B.T.N. Ngoc, K.S. Yang, M. Kojima, Y.A. Kim, Y.J. Kim, M. Endo, S.C. Yang, Self-sustained thin webs consisting of porous carbon nanofibers for supercapacitors via the electrospinning of polyacrylonitrile solutions containing zinc chloride, Adv. Mater. 19 (2007) 2341–2346.
[35] Y.P. Huang, Y.E. Miao, L.S. Zhang, W.W. Tjiu, J.S. Pan, T.X. Liu, Synthesis of few-layered MoS_2 nanosheet-coated electrospun SnO_2 nanotube heterostructures for enhanced hydrogen evolution reaction, Nanoscale 6 (2014) 10673–10679.
[36] Y.E. Miao, H. Zhu, D. Chen, R.Y. Wang, W.W. Tjiu, T.X. Liu, Electrospun fibers of layered double hydroxide/biopolymer nanocomposites as effective drug delivery systems, Mater. Chem. Phys. 134 (2012) 623–630.
[37] Y.E. Miao, G.N. Zhu, H.Q. Hou, Y.Y. Xia, T.X. Liu, Electrospun polyimide nanofiber-based nonwoven separators for lithium-ion batteries, J. Power Sources 226 (2013) 82–86.
[38] Y.E. Miao, S.X. He, Y.L. Zhong, Z. Yang, W.W. Tjiu, T.X. Liu, A novel hydrogen peroxide sensor based on Ag/SnO_2 composite nanotubes by electrospinning, Electrochim. Acta 99 (2013) 117–123.
[39] Y.P. Huang, Y.E. Miao, S.S. Ji, W.W. Tjiu, T.X. Liu, Electrospun carbon nanofibers decorated with Ag-Pt bimetallic nanoparticles for selective detection of dopamine, ACS Appl. Mater. Interfaces 6 (2014) 12449–12456.
[40] Y.P. Huang, Y.E. Miao, T.X. Liu, Electrospun fibrous membranes for efficient heavy metal removal, J. Appl. Polym. Sci. (2014) , doi:http://dx.doi.org/10.1002/app.40864.
[41] Q.H. Guo, X.P. Zhou, X.Y. Li, S.L. Chen, A. Seema, A. Greiner, H.Q. Hou, Supercapacitors based on hybrid carbon nanofibers containing multiwalled carbon nanotubes, J. Mater. Chem. 19 (2009) 2810–2816.
[42] E. Kenawy, F.I. Abdel-Hay, M.H. El-Newehy, G.E. Wnek, Processing of polymer nanofibers through electrospinning as drug delivery systems, Mater. Chem. Phys. 113 (2009) 296–302.
[43] W.J. Li, C.T. Laurencin, E.J. Caterson, R.S. Tuan, F.K. Ko, Electrospun nanofibrous structure: a novel scaffold for tissue engineering, J. Biomed. Mater. Res. 60 (2002) 613–621.
[44] C. Kim, K.S. Yang, Electrochemical properties of carbon nanofiber web as an electrode for supercapacitor prepared by electrospinning, Appl. Phys. Lett. 83 (2003) 1216–1218.
[45] H.L. Wang, Q.M. Gao, J. Hu, Asymmetric capacitor based on superior porous Ni-Zn-Co oxide/hydroxide and carbon electrodes, J. Power Sources 195 (2010) 3017–3024.
[46] J.W. Lee, T. Ahn, D. Soundararajan, J.M. Ko, J. Kim, Non-aqueous approach to the preparation of reduced graphene oxide/alpha-$Ni(OH)_2$ hybrid composites and their high capacitance behavior, Chem. Commun. 47 (2011) 6305–6307.
[47] R.Z. Ma, J.B. Liang, K. Takada, T. Sasaki, Topochemical synthesis of Co-Fe layered double hydroxides at varied Fe/Co ratios: unique intercalation of triiodide and its profound effect, J. Am. Chem. Soc. 133 (2011) 613–620.
[48] J. Pu, Y. Tong, S.B. Wang, E.H. Sheng, Z.H. Wang, Nickel-cobalt hydroxide nanosheets arrays on Ni foam for pseudocapacitor applications, J. Power Sources 250 (2014) 250–256.
[49] Z.R. Chang, Y.J. Zhao, Y.C. Ding, Effects of different methods of cobalt addition on the performance of nickel electrodes, J. Power Sources 77 (1999) 69–73.
[50] F. Zhang, C.Z. Yuan, X.J. Lu, L.J. Zhang, Q. Che, X.G. Zhang, Facile growth of mesoporous Co3O4 nanowire arrays on Ni foam for high performance electrochemical capacitors, J. Power Sources 203 (2012) 250–256.
[51] H.L. Wang, Q.M. Gao, L. Jiang, Facile approach to prepare nickel cobaltite nanowire materials for supercapacitors, Small (2011) 2454–2459.